# Equilibrium Shape of Steps and Islands on Polar II-VI Semiconductors Surfaces

D. Martrou, J. Eymery, and N. Magnea

*CEA Grenoble, Département de Recherche Fondamentale sur la Matière Condensée, 17 Avenue des Martyrs, 38054 Grenoble Cedex 9, France*

(Received 29 April 1999)

Scanning tunneling microscopy studies of (001) surfaces of partially ionic II-VI compounds show novel surface structures with step and 2D island edges aligned along the ⟨100⟩ crystallographic directions. We propose a simplified model incorporating electrostatic interactions in the calculation of the energy of charged steps that could explain why the free energy of ⟨100⟩ steps lies below that of the [110] and [1$\bar{1}$0] steps. The energetics of the vicinal surfaces is strongly influenced by this original effect which makes possible the fabrication of staircase and checkerboard templates for growing self-organized nanostructures.

PACS numbers: 68.35.Bs, 61.16.Ch, 68.35.Md, 72.80.Ey

After epitaxial growth in conditions where kinetic equilibrium is established, i.e., low growth rate and high temperature, well defined morphological structures appear on the surfaces of solids. On a perfectly flat surface, the main structures are two dimensions (2D) islands of atomic height, whose shape is controlled by the nature of the chemical bonding—metallic, covalent, or ionic—between the atoms and the way they rearrange on the surface. These reconstructions result from the relaxation of the surface atoms from their bulk position and/or the rehybridization of occupied atomic orbitals [1]. For the (001) surface of semiconductors growing in the diamond or in the zinc blende (ZB) structure with a predominantly covalent bond, the surface atoms pair up to reduce the number of unsatisfied bonds. This anisotropic bonding strongly affects the kinetics and energetics of 2D island formation.

In silicon, the (001) surface reconstruction is alternatively ($2 \times 1$) and ($1 \times 2$) and the "growth shapes" are islands elongated in the [110] and [1$\bar{1}$0] directions as a result of the strong preference of atoms to stick at the ends of the Si dimer rows rather than at the sides [2]. The "equilibrium shapes" of the islands are made of rectangles with ⟨110⟩ edges and an aspect ratio close to 3, reflecting here the free energy ratio between the [110] and the [1$\bar{1}$0] steps [3]. The surface stress resulting from the reconstruction anisotropy is responsible for the elastic interactions between monatomic steps [4]. On the polar gallium arsenide (001) surface, the most commonly observed reconstruction is ($2 \times 4$) or $c(2 \times 8)$ involving As dimers. At equilibrium, the islands are anisotropic structures with their long edge in the [1$\bar{1}$0] direction, the $2\times$ direction [5]. It has been shown that the ionicity of the Ga-As bond (Philips' ionicity $f_i = 0.3$) [6] affects, through dipolar interactions, the short range kink interactions [7] and also the step coupling [8] without modifying the surface morphology from that seen on the purely covalent Si surface.

On II-VI zinc blende semiconductors with a stronger ionicity ($0.5 < f_i < 0.7$), the bonding loses a part of its strength and directionality and large electronic dipoles are created due to the charge transfer between anions and cations. Thus elastic interactions which were dominant at the surface of a covalent material are weakened and, in counterpart, isotropic Coulomb interactions will contribute more to the surface energy which in the case of the polar (001) face is stabilized only by substantial reconstructions [9]. The question is as follows: to what extent are the epitaxial growth, the relaxation, and the morphology of these II-VI semiconductor surfaces affected by the strong ionicity of their atomic bonding?

This question is addressed in this Letter by studying, by scanning tunneling microscopy (STM), the polar (001) surface of tellurides obtained by molecular beam epitaxy (MBE). The materials ZnTe and CdTe used in this study keep the same fourfold atomic coordination as Si or GaAs but have an ionicity factor of 0.609 and 0.717, respectively [6]. A key result of our analysis is the observation of isotropic islands with (100) edges for the tellurium rich ($2 \times 1$) surfaces showing that the free energy of the ⟨100⟩ steps is lower than that of the ⟨110⟩ steps. We postulate that this unusual configuration for ZB materials can be attributed to the electrostatic interactions along the charged steps. As a consequence, the epitaxial growth on vicinal CdTe surfaces leads to a self-organization of steps in a staircase or checkerboard array totally different from anything commonly seen on Si or GaAs.

The experiments are performed in an ultrahigh vacuum system with facilities for epitaxy of II-VI compounds and STM imaging. The layers are grown by MBE, in the temperature range $T_{\text{sub}} = 300-330\,^{\circ}\text{C}$. Because of the low bonding energy of II-VI compounds, we consider that at these temperatures, the surface has reached a thermal quasiequilibrium, and that the structures observed by STM have equilibrium shapes.

After cooling down to 250 °C, under the thermal beam of $Te_2$ molecules, the samples are transferred through a gate valve to the STM apparatus. The STM images are obtained at a voltage of 2–2.5 V and a tunnel current of 100 pA.

 0031-9007/99/83(12)/2366(4)$15.00 

The samples are illuminated in order to photogenerate carriers in the undoped epilayers and substrate. The borders of the STM images are aligned along the [110] and [1$\bar{1}$0] directions identified by the orientation of cleaved edges and of the (2 × 1) Te reconstruction.

The wide scale STM image of Fig. 1a was recorded after deposition of 50 nm of CdTe at $T_{sub}$ = 300 °C on a nominally flat substrate, followed by a 5 min annealing under a Te flux of 1 monolayer/s (1 ML/s) at $T_{sub}$ = 330 °C. The (001) CdTe surface is clean and flat with wide monomolecular terraces. The local misorientations of the (001) surface result in random steps and "giant" kinks which are all oriented along the ⟨100⟩ directions.

If the annealing is performed at $T_{sub}$ = 320 °C under a low Te flux (0.35 ML/s) the equilibrium between the CdTe surface and the vapor phase is displaced towards sublimation. The STM image of Fig. 1b reveals holes with a depth of one CdTe monolayer (3.24 Å). These "negative" 2D islands are attributed to a local thermal etching of the terraces due to the congruent sublimation of CdTe. The edges of these isotropic holes are also oriented preferentially along the ⟨100⟩ directions. The similarity of the steps orientation observed either after deposition or after sublimation is a sufficient condition to suppose that the ⟨100⟩ steps are near equilibrium.

The last image 1c has been obtained after deposing a fractional monolayer of CdTe on a smoothed CdTe (001) surface by atomic layer epitaxy at $T_{sub}$ = 300 °C. This growth technique is a means of producing a regular array of monomolecular 2D islands with a self-regulated coverage close to 0.5 [10]. The size of the islands increases with the temperature of deposition but they always keep square or rectangular shapes with ⟨100⟩ edges.

High resolution images revealing the reconstruction of the Te terminated surfaces and the atomic structure of the monomolecular islands are shown in Fig. 2. For the Te rich surface with the (2 × 1) reconstruction, we observe on Fig. 2a the $Te_2$ dimer rows parallel to the [110] direction despite the presence of $Te_2$ diatomic molecules physisorbed during cooling down. The STM image is in close agreement with the relaxed structure calculated by *ab initio* method [11] and shown below Fig. 2a. The result of the calculation confirms the small outward relaxation, the large surface corrugation of the Te terminated surface, and the $\pi$-like bonding of the $Te_2$ dimer which explains the difficulty to observe with STM the two Te atoms in a dimer. The key feature of this surface appearing on Fig. 2b is that the borders of the island do not follow the surface symmetry but are oriented at 45° from the ⟨110⟩ principal axis of the reconstruction forming ⟨100⟩ edges. The high resolution image (Fig. 2b) shows that these edges are, in fact, made of a staggering of elementary kinks aligned along the [110] (*B* kinks) and the [1$\bar{1}$0] (*A* kinks) axis.

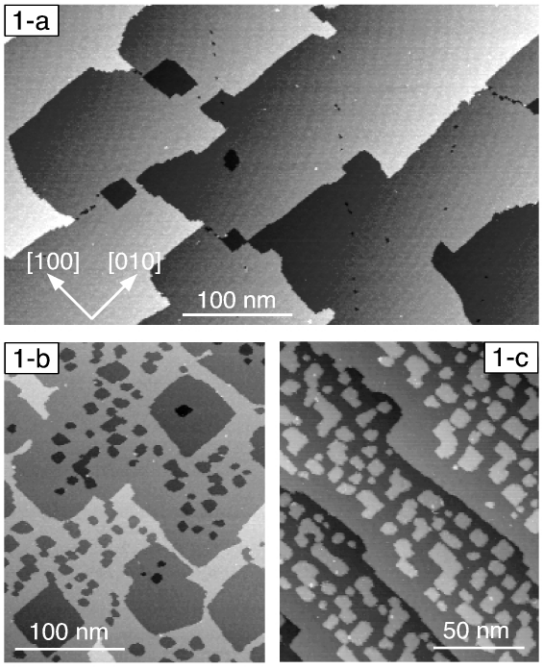


FIG. 1. Large scale STM images of CdTe (001) surface: (a) grown at 300 °C and smoothed at 330 °C under a 1.0 ML/s Te flux; (b) sublimated at 320 °C under a 0.35 ML/s Te flux; (c) covered at 300 °C by 1/2 ML of CdTe using atomic layer epitaxy. The steps edges are parallel to the ⟨100⟩ directions indicated in (a).

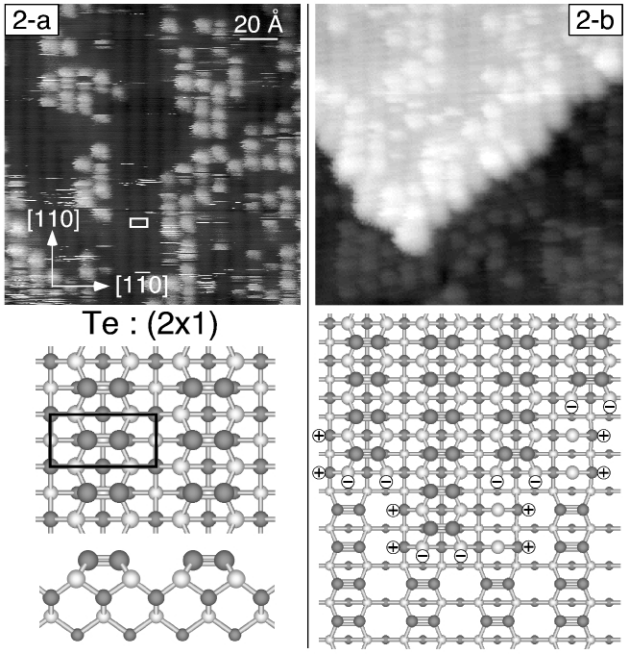


FIG. 2. High resolution STM images of the Te rich surface. (a) Te (2 × 1) reconstruction, the calculated top and cross section views are shown below the experimental image. Cd and Te atoms are, respectively, white and black balls. (b) Monomolecular island and atomic model showing the charged atoms on step edges.

The main conclusion of this analysis is that ⟨100⟩ steps of the $(2 \times 1)$ Te rich surface of CdTe have a formation energy which is lower than that of [110] ($B$ step) and $[1\bar{1}0]$ ($A$ step) edges. On standard Si (001) surfaces this is the opposite while the symmetry and the atomic structure of the reconstructed (001) surface are similar. The exception is observed only on ultraflat Si substrates where the straight $A$ and $B$ steps develop coherent long wavelength undulations ($10^3$ to $10^4$ nm) to reduce elastic energy [12]. We think that the unusual behavior of Te based II-VI materials can be found in the large ionicity of the bonding which results in charged steps. From this point of view, the CdTe (001) surface behaves more like MgO or NaCl ionic crystal surfaces where only ⟨100⟩ steps with edge formed of a line of anions and cations pairs are stable [13].

In order to elucidate the origin of the forces that stabilize the ⟨100⟩ configuration, the contribution of the step energy $E(n)$ to the total energy of a CdTe island deposed on a (001) CdTe surface is evaluated as a function of the number $n$ of atoms forming "100" and "110" square islands. Their edge and charge configurations are depicted schematically in Fig. 3. Our simplified calculation is based on an extension of the model of Tersoff and Tromp [14] which gives an analytical value of $E(n)$ for a pseudomorphic island. In this model the island energy is the sum of the extra surface energy, the local step energy, and the energy change due to step relaxation where we add the Coulombic interactions between the charges located at the borders of the islands. We assume that these effective charges arise from the deviation of the electronic distribution at the step from that of the flat surface. For the $B$-type steps on the Te rich surface, the Te atom sitting at the edge is coordinated with three Cd atoms instead of four in the bulk. In a purely ionic model, this is equivalent to a net positive charge of $(1/4)q^*$ compared to the effective charge $q^*$ equal to 0.33 electron in bulk CdTe [6]. For the $A$-type steps this is the Cd atom which carries a net negative charge of $(-1/4)q^*$. Then, the interactions between these static charges lead to the Coulomb energy $E_C(n) = M(n)^{ijk}(q^*/4)^2/(4\pi\epsilon_0 d[110])$, where $d[110] = 4.54$ Å is the distance between the charged atoms along the ⟨110⟩ axis. $M(n)^{ijk}$ is a 2D Madelung factor calculated numerically for the two charge configurations shown in Fig. 3. The interactions of these extra charges with the surface and bulk dipolar charges are at first order smaller and identical for the two configurations. As mentioned by Lelarge *et al.* [8], the dipolar interactions will dominate the long range step-step interactions.

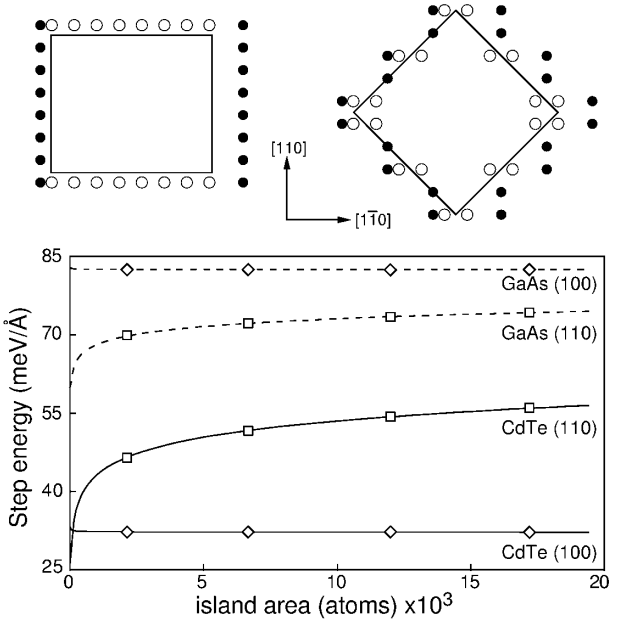


FIG. 3. Variation of the step energy vs the number of atoms forming an island calculated for CdTe and GaAs. The calculation is made for the "110" (□) and "100" (◇) steps and charges configuration depicted above the curves; ●, "positively" charged Te atoms; ○, "negatively" charged Cd atoms.

The other contributions $E_{el}(n)$ to the total energy $E(n)$ involves the line tension resulting from the broken bonds at the steps and the elastic relaxation induced by the long range interaction between step edges of the islands [4,14,15]. The relaxation term can be neglected for homoepitaxy of binary compounds with double steps due to the absence of alternating surface stress domains [4]. For heteroepitaxy, its contribution depends on the misfit between the deposed islands and the substrate [14]. The line tension, supposed to be proportional to the cohesive energy of the bulk material, is estimated for CdTe around 27 meV/Å by scaling with the GaAs value [15]. For ideally square islands, which means that we do not consider a possible energy anisotropy of $A$ and $B$ steps [16], $E_{el}(n)$ is a factor of $\sqrt{2}$ higher for the 100 than for the 110 configuration due to the difference in the number of broken bonds. For the 110 configuration, the corner energy can be disregarded because we consider only elementary kinks of length $2d[110]$ [17].

The plot of $E(n) = E_{el}(n) + E_C(n)$, represented in Fig. 3, shows that the 100 island configuration is stabler than the 110 for CdTe islands on CdTe. This is because the gain in energy of the 100 configuration due to the Coulomb interactions [$E_C(n)$ is negative] is greater than the elastic energy cost due to a larger step length. For the 110 configuration, the step length is shorter but $E_C(n)$ is now positive and increases rapidly with $n$ so that islands with straight ⟨110⟩ steps become unstable for $n > 30$.

The same estimate of $E(n)$ made for GaAs by taking a line tension of 55 meV/Å [15] and $q^* = 0.2$ [6] is shown in Fig. 3. Because GaAs is stiffer and less ionic than CdTe, elasticity is predominant and the ⟨110⟩ steps are always stabler than the ⟨100⟩. The small Coulomb energy affects only the short range kink-kink interactions [7] but not the overall shape of the islands which mimic more or less the symmetry of the surface reconstruction. For Si,

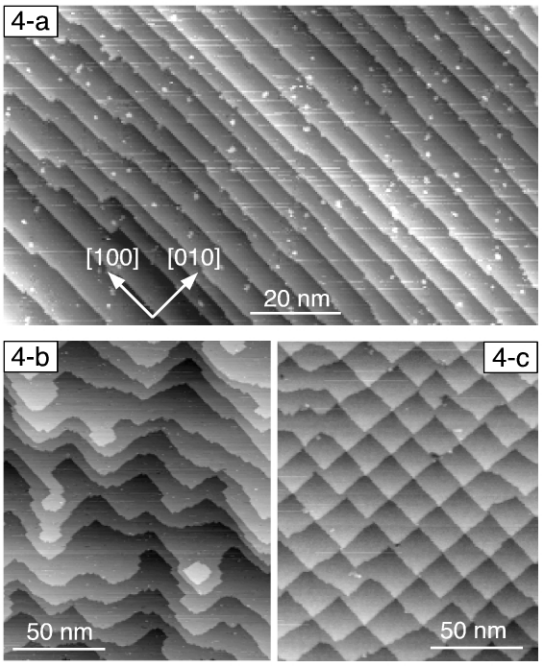


FIG. 4. Large scale STM images of CdTe on vicinal surfaces: (a) *C* type organized in a staircase. (b) *A* type after growth at 300 °C and 0.2 ML/s. (c) *A* type self-organized in a checkerboard after growth at 330 °C and 0.1 ML/s.

where $q^* = 0$, the kink-kink interactions disappear and the line tension plays the major role so that anisotropic islands with [110] and [1$\bar{1}$0] edges are observed.

The large ionicity of the bonding of CdTe has important consequences for the growth on vicinal surfaces where the knowledge acquired on Si and GaAs cannot be transferred directly to CdTe (001) surfaces. For thermodynamic parameters favoring a step flow growth mechanism, straight and equally spaced steps are expected on the CdTe *C*-type surface with the surface normal tilted towards [100], instead of the *A*-type surface (tilted towards [110]) as in GaAs [18]. This is demonstrated on Fig. 4a showing, after epitaxy, an STM image of a *C*-type surface of CdTe with a miscut angle of 1°. The ⟨100⟩ steps are parallel and regularly spaced with only microroughness corresponding to atomic kinks. For *A*- or *B*-type CdTe surface, the ⟨110⟩ miscut axis does not correspond to the energetically most favorable steps. Thus, the steps and terraces are extremely disordered as shown in Fig. 4b obtained on an *A*-type surface after molecular beam epitaxy at $T_{\text{sub}} = 300$ °C and growth rate of 0.2 ML/s. Because of the low energy of formation of ⟨100⟩ steps, macrokinks with [100] axis are easily excited forming sawtooth structures. If now the growth rate on an *A*-type surface is reduced below 0.1 ML/s and the temperature raised to 330 °C, a quasiequilibrium state is reached consisting of a self-organized checkerboard array of square terraces as shown in Fig. 4c. A plausible origin of the checkerboard (i.e., the dephasing of the sawtooths), which will be detailed in a forthcoming paper, is the existence of long range electrostatic interactions between dissymmetric ⟨100⟩ edges.

In conclusion, we have observed in materials with a fourfold coordination, but with a bonding that is dominated by ionic interactions, novel step configurations and islands shapes. The 2D islands are isotropic with ⟨100⟩ edges and do not necessarily reproduce the symmetry of the surface reconstruction as in covalent semiconductors. We suggest that in II-VI compounds, the softening of the bond weakens the anisotropic elastic interactions which dominate the energetics of surface structures in Si and to a lesser extent GaAs, but strengthens the isotropic Coulomb interaction. A simple calculation of each contribution to the edge energy of CdTe islands indicates that the energy to form a ⟨100⟩ edge (made of *A* and *B* elemental kinks) is lower than for ⟨110⟩ edges if static charges exist at step edges. The same behavior is also expected in ZnSe ($f_i = 0.63$; $q^* = 0.34$). These experimental results have been used to find out and prepare the vicinal surfaces suitable for growing self-organized quantum nanostructures. This is the staircase formed on *C*-type vicinal surface which will be the template for fabrication of quantum wires, while the *A*-type surface organized in a checkerboard array appears as the best template for growing quantum boxes [19].

[1] M. G. Lagally, Phys. Today **46**, No. 11, 24 (1993).
[2] Y. W. Mo and M. G. Lagally, Surf. Sci. **248**, 313 (1991).
[3] Y. W. Mo *et al.*, Phys. Rev. Lett. **63**, 2392 (1989).
[4] O. L. Alerhand *et al.*, Phys. Rev. Lett. **61**, 1973 (1988).
[5] M. D. Pashley, K. W. Haberern, and J. M. Gaines, Appl. Phys. Lett. **58**, 406 (1991); Phys. Rev. B **40**, 10 481 (1989).
[6] J. C. Philips, *Bonds and Bands in Semiconductors* (Academic Press, New York, 1973).
[7] E. J. Heller and M. G. Lagally, Phys. Rev. Lett. **71**, 743 (1993).
[8] F. Lelarge, Z. Z. Wang, A. Cavanna, F. Laruelle, and B. Etienne, Europhys. Lett. **39**, 97 (1997).
[9] C. Noguera, *Physics and Chemistry of Oxide Surface* (Cambridge University Press, Cambridge, 1996).
[10] J. M. Hartmann, G. Feuillet, M. Charleux, and H. Mariette, J. Appl. Phys. **79**, 3035 (1996).
[11] S. Gundel *et al.*, Phys. Rev. B **59**, 23 (1999); **59**, 15 261 (1999).
[12] R. M. Tromp and M. C. Reuter, Phys. Rev. B **47**, 7598 (1993).
[13] Y. W. Tsang and L. M. Falicov, Phys. Rev. B **12**, 2441 (1975).
[14] J. Tersoff and R. M. Tromp, Phys. Rev. Lett. **70**, 2782 (1993).
[15] C. Priester and M. Lannoo, Phys. Rev. Lett. **75**, 93 (1995).
[16] D. J. Chadi, Phys. Rev. Lett. **59**, 1691 (1987).
[17] H. J. W. Zandvliet *et al.*, Phys. Rev. **45**, 5965 (1992).
[18] P. R. Pukite *et al.*, J Cryst. Growth **95**, 269 (1989).
[19] D. Martrou and N. Magnea, J. Cryst. Growth **201**, 101 (1999).